International Journal of Fracture **96:** 203–214, 1999.
© 1999 *Kluwer Academic Publishers. Printed in the Netherlands.*

Singularity characteristics for a lip-shaped crack subjected to remote biaxial loading

YU QIAO and YOUSHI HONG*
Lab for Nonlinear Mechanics of Continuous Media, Institute of Mechanics, Chinese Academy of Sciences, Beijing 100080, China

Received 16 July 1997; accepted in revised form 2 April 1999

Abstract. In this paper, the conformal mapping method was adopted to solve the problem of an infinite plate containing a central lip-shaped crack subjected to remote biaxial loading. A kind of leaf-shaped configuration was also constructed in order to solve the problem. The analytical result showed that the singularity order of the stress field at the tip of a lip-shaped crack remains $-1/2$, despite the difference in notch-crack width.

Key words: Singularity order, lip-shaped crack, leaf-shaped notch, conformal mapping, complex stress function.

1. Introduction

According to Williams (1952; 1957) and Irwin (1957), the singularity order of the stress field at the tip of a planar crack loaded under plane-strain mode I condition is $-\frac{1}{2}$, and the stress intensity factor K is introduced to characterize the stress concentration. These concepts have become the basis of Linear Elastic Fracture Mechanics (LEFM), which has been widely used in theoretical analyses and engineering applications.

It is noted that there are some reasons for omitting terms with a higher singularity order in the LEFM derivations. These reasons (Hui, 1995) are:

(1) the strain energy in the region of the crack tip must be bounded;
(2) the displacement in the region of the crack tip must be bounded;
(3) the uniqueness of elastic solutions is lost if higher-order singular solutions are allowed; and
(4) the solution for the stress field in the vicinity of an elliptical hole, *in the limit as* the aspect ratio goes to infinite, does not have such higher-order singular temrs.

Some recent studies (Hui, 1995; Zhao, 1996) argued that the four reasons are not convincing, and that more singular terms should be included. It has also been argued that the singularity order of the stress field at the tip of a propagating crack may be higher than $-\frac{1}{2}$ (Wang, 1992; Prakash et al., 1992). Note that the above analyses are focused on ideal geometric cracks, i.e. the crack width is zero. However, in real physical circumstances, a crack is always of a certain width.

A kind of lip-shaped crack exists during the damage process of some materials, and the stress field is controlled by such a crack. It is also known that the stress distribution ahead of a notch is a vital factor in fatigue investigation and failure analysis, since cracks are prone to initiate from a notch root, prior to final fracture. The analytical solutions to a notch crack are

* Author for correspondence.

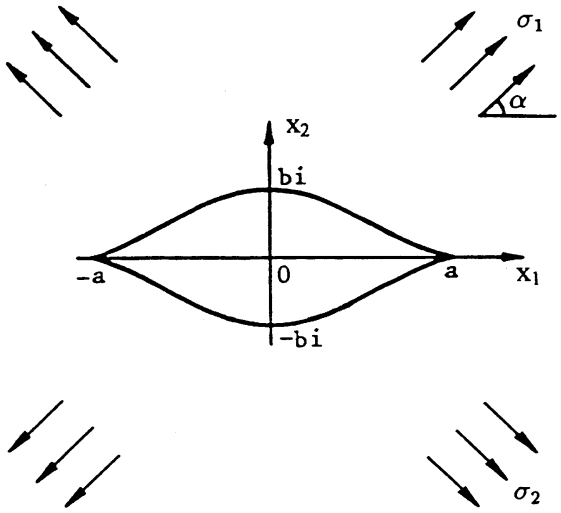

Figure 1. Infinite plate containing a central lip-shaped notch under remote biaxial loading.

difficult to obtain and they are sometimes shown as lip-shaped cracks as illustrated in Figure 1 (Hong et al., 1991). Various approaches based on LEFM have been applied to deal with the notch-crack problem (Bowie, 1956; Schijve, 1982; Xiao et al., 1985; Baskes, 1975), and many of them are numerical methods to calculate the stress field at the tip of a notch crack.

In this paper, a kind of lip-shaped crack with a dimension in width is studied. The complex stress function method developed by Muskhelishvili (1954) is adopted to solve the problem of an infinite plate containing a central lip-shaped crack subjected to remote biaxial loading. In order to solve the problem, a leaf-shaped profile is constructed, which is similar to the lip-shaped contour but has round tips so as to allow for the integral operation during the theoretical derivations. Finally, the singularity order of the stress field at the tip of the lip-shaped crack with a crack width is derived.

2. Basic equations

Figure 1 shows an infinite thin plate with a central lip-shaped crack subjected to remote biaxial loading. One may transform the lip-shaped profile on the z-plane to a unit circle on the ζ-plane (Figure 2) via the following conformal mapping formula

$$z = \omega_0(\varsigma) = \tfrac{1}{2}ar\left[\varsigma + \frac{m}{\varsigma} + \frac{\varsigma}{r^2(\varsigma^2 + m)}\right], \tag{1}$$

where a is the half-length of the lip-shaped profile, $m = a/b - \sqrt{1 + (a/b)^2}$, b is the half-width of the lip-shaped profile, and $r = 1/(1 + m)$. Because of the difficulty in dealing with the singular points in the derivation of the complex stress function, which was overlooked in the previous investigation (Hong et al., 1991), we further construct the conformal mapping formula

$$z = \omega(\varsigma) = \tfrac{1}{2}ar\left[\varsigma + \frac{m}{\varsigma} + \frac{\varsigma}{r^2(\varsigma^2 + m)}\right] + a\xi\varsigma \tag{2}$$

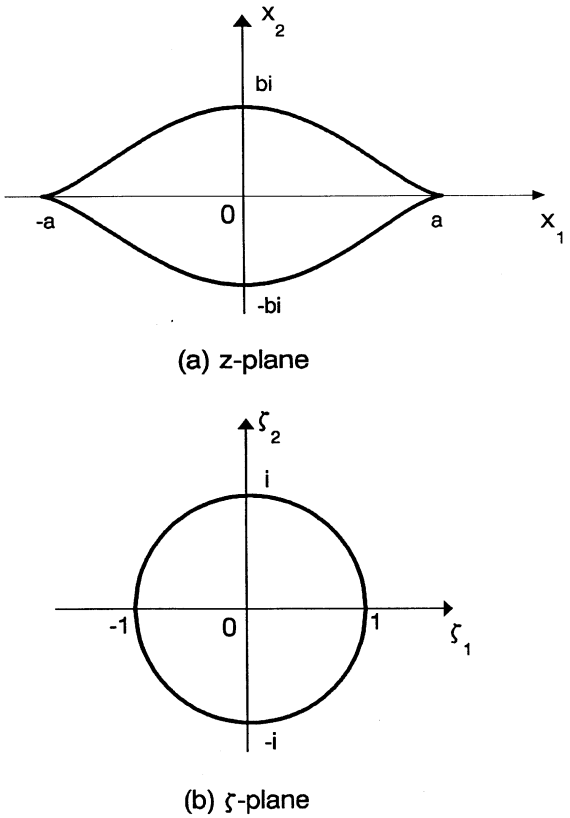

Figure 2. Mapping a lip-shaped profile in z-plane (a) onto a unit circle in ζ-plane (b).

to transform a leaf-shaped instead of a lip-shaped profile on the z-plane to a unit circle on the ζ-plane, where ξ is a shape factor. The leaf-shaped profile possesses smooth tips instead of sharp ones, which enable it to be integrated around the profile boundary. It is obvious that when ξ tends to zero, Equation (2) reduces to Equation (1). As a result, the leaf-shaped profile tends to the lip-shaped profile. Thus, the stress field near the tips of a lip-shaped crack can be obtained by calculating the stress field of a leaf-shaped profile first, and then letting ξ tend to zero. Figures 3(a)–(d) illustrate how the leaf-shaped contour transforms to the lip-shaped profile with a decrasing value of ξ.

According to the theory developed by Muskhelishvili (1954), the general form of complex stress functions for an infinite planar problem on the ζ-plane are

$$\phi(\varsigma) = \Gamma R\varsigma - \frac{X + iY}{2\pi(1+\kappa)} \ln \varsigma + \phi_0(\varsigma), \tag{3}$$

$$\psi(\varsigma) = \Gamma_1 R\varsigma + \frac{\kappa(X - iY)}{2\pi(1+\kappa)} \ln \varsigma + \psi_0(\varsigma), \tag{4}$$

where X and Y are the resultant forces on the crack boundary, Γ and Γ_1 are constants depending on the remote loading conditions, $R = \frac{1}{2}ar + a\xi$, $\phi_0(\varsigma)$ and $\psi_0(\varsigma)$ are holomorphic for $|\zeta| > 1$, and

$$\phi_0(\infty) = \psi_0(\infty) = 0. \tag{5}$$

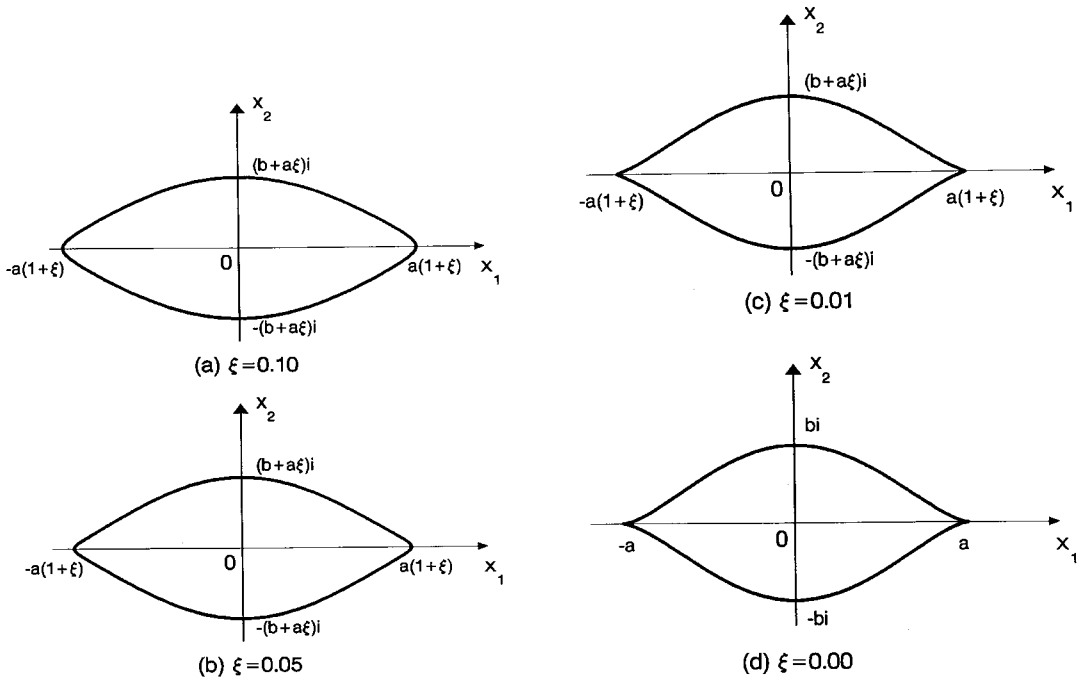

Figure 3. Leaf-shaped profile tending to lip-shaped crack as ξ reduces to zero.

For plane stress

$$\kappa = \frac{3-\nu}{1+\nu},$$

where ν is Poisson's ratio.

Let γ be the circumference of the unit circle of the ζ-plane with $\eta = \mathrm{e}^{i\theta}$. On γ, according to (3) and (4), the complex stress functions have the forms

$$\phi(\eta) = \Gamma R\eta - \frac{X+iY}{2\pi(1+\kappa)} \ln \eta + \phi_0(\eta), \tag{6}$$

$$\psi(\eta) = \Gamma_1 R\eta + \frac{\kappa(X-iY)}{2\pi(1+\kappa)} \ln \eta + \psi_0(\eta). \tag{7}$$

The boundary condition on the ζ-plane has the form

$$\phi(\eta) + \frac{\omega(\eta)}{\overline{\omega'(\eta)}} \overline{\phi'(\eta)} + \overline{\psi(\eta)} = f, \tag{8}$$

where $f = i\int_0^s (X_n + iY_n)\,\mathrm{d}s$, with X_n and Y_n being the resultant amounts of the positive normal stress on the element ds of the boundary. In this paper, '$\overline{\ }$' denotes conjugate operation, and '$'$' denotes differential operation. Substituting (6) and (7) into (8), one may obtain the boundary conditions for the complex stress functions

$$\phi_0(\eta) + \frac{\omega(\eta)}{\overline{\omega'(\eta)}} \overline{\phi_0'(\eta)} + \overline{\psi_0(\eta)} = f_0, \tag{9}$$

$$\overline{\phi_0(\eta)} + \frac{\overline{\omega(\eta)}}{\omega'(\eta)}\,\phi_0'(\eta) + \psi_0(\eta) = \overline{f_0}, \tag{10}$$

where

$$f_0 = f - \Gamma R\eta + \frac{X+iY}{2\pi}\ln\eta - \frac{\omega(\eta)}{\overline{\omega'(\eta)}}\left[\overline{\Gamma}R - \frac{X-iY}{2\pi(1+\kappa)}\eta\right] - \overline{\Gamma}_1 R\frac{1}{\eta}, \tag{11}$$

$$\overline{f_0} = \overline{f} - \overline{\Gamma}R\frac{1}{\eta} - \frac{X-iY}{2\pi}\ln\eta - \frac{\overline{\omega(\eta)}}{\omega'(\eta)}\left[\Gamma R - \frac{X+iY}{2\pi(1+\kappa)}\frac{1}{\eta}\right] - \Gamma_1 R\eta. \tag{12}$$

Equations (3), (4) and (9)–(12) are the basic equations of the problem.

3. Complex stress functions and the singularity order

When a plate with a central leaf-shaped notch is subjected to remote biaxial loading without rotation, the corresponding remote boundary conditions are

$$\Gamma = \overline{\Gamma} = \tfrac{1}{4}(\sigma_1 + \sigma_2), \tag{13}$$

$$\Gamma_1 = -\tfrac{1}{2}(\sigma_1 - \sigma_2)\,\mathrm{e}^{-2i\alpha}, \tag{14}$$

where σ_1 and σ_2 are the remote principal stresses due to external loading, α is the angle between the direction of σ_1 and the axis $0x_1$. The boundary conditions on the notch surface are

$$f = 0 \tag{15}$$

and

$$X + iY = 0. \tag{16}$$

Substituting (13)–(16) into (11) and (12), we may have

$$f_0 = -\tfrac{1}{4}R(\sigma_1+\sigma_2)\left[\eta + \frac{\omega(\eta)}{\overline{\omega'(\eta)}}\right] + \tfrac{1}{2}R(\sigma_1-\sigma_2)\frac{1}{\eta}\,\mathrm{e}^{2i\alpha}, \tag{17}$$

$$\overline{f_0} = -\tfrac{1}{4}R(\sigma_1+\sigma_2)\left[\frac{1}{\eta} + \frac{\overline{\omega(\eta)}}{\omega'(\eta)}\right] + \tfrac{1}{2}R(\sigma_1-\sigma_2)\eta\,\mathrm{e}^{-2i\alpha}, \tag{18}$$

where

$$\frac{\omega(\eta)}{\overline{\omega'(\eta)}} = \frac{(1+m\eta^2)^2[r^2m(\eta^2+m)+\eta^2+(r+2\xi)r\eta^2(\eta^2+m)]}{r\eta(\eta^2+m)[r(1-\eta^2)(1-m\eta^2)(1-m^2\eta^2)+2\xi(1+m\eta^2)^2]}, \tag{19}$$

$$\frac{\overline{\omega(\eta)}}{\omega'(\eta)} = \frac{\eta(m+\eta^2)^2\{[r^2m(1+m\eta^2)+1]\eta^2 + r(r+2\xi)(1+m\eta^2)\}}{r(1+m\eta^2)[r(\eta^2-1)(\eta^2-m)(\eta^2-m^2)+2\xi(\eta^2+m)^2\eta^2]}. \tag{20}$$

Equations (19) and (20) are derived from (2).

Equations (19) and (20) show that $\omega(\varsigma)/\overline{\omega'}(1/\varsigma)\overline{\phi_0'}(1/\varsigma)$ is holomorphic inside γ except at $\pm\sqrt{-m}$, $\overline{\omega}(1/\varsigma)/\omega'(\varsigma)\phi_0'(\zeta)$ is holomorphic outside γ except at $\pm 1/\sqrt{-m}$. So that, according to the Cauchy integral theorem (for $|\zeta| > 1$)

$$\begin{aligned}
&\frac{1}{2\pi i}\int_\gamma \frac{\omega(\eta)}{\overline{\omega'(\eta)}}\overline{\phi_0'(\eta)}\frac{\mathrm{d}\eta}{\eta-\varsigma} \\
&\quad = \frac{1}{2\pi i}\int_\gamma \frac{\omega(\eta)}{\overline{\omega'(\eta)}}\overline{\phi_0'}\left(\frac{1}{\eta}\right)\frac{\mathrm{d}\eta}{\eta-\varsigma} \\
&\quad = -G_1(\varsigma) - G_2(\varsigma) = -\frac{M_0}{2}\left[\frac{\overline{\phi_0'}\left(\frac{1}{\sqrt{-m}}\right)}{\varsigma-\sqrt{-m}} + \frac{\overline{\phi_0'}\left(\frac{-1}{\sqrt{-m}}\right)}{\varsigma+\sqrt{-m}}\right], \qquad (21)
\end{aligned}$$

$$\begin{aligned}
&\frac{1}{2\pi i}\int_\gamma \frac{\overline{\omega(\eta)}}{\omega'(\eta)}\phi_0'(\eta)\frac{\mathrm{d}\eta}{\eta-\varsigma} \\
&\quad = -\frac{\overline{\omega}(1/\varsigma)}{\omega'(\varsigma)}\phi_0'(\varsigma) + H_1(\varsigma) + H_2(\varsigma) \\
&\quad = -\frac{\overline{\omega}(1/\varsigma)}{\omega'(\varsigma)}\phi_0'(\varsigma) - \frac{M_0}{2m}\left[\frac{\phi_0'\left(\frac{1}{\sqrt{-m}}\right)}{\varsigma-\frac{1}{\sqrt{-m}}} - \frac{\phi_0'\left(\frac{-1}{\sqrt{-m}}\right)}{\varsigma+\frac{1}{\sqrt{-m}}}\right], \qquad (22)
\end{aligned}$$

where G_1 and G_2 are respectively the principal parts of $\omega(\varsigma)/\overline{\omega'}(1/\varsigma)\overline{\phi_0'}(1/\varsigma)$ at $\sqrt{-m}$ and $-\sqrt{-m}$; H_1 and H_2 are respectively the principal parts of $\overline{\omega}(1/\varsigma)/\omega'(\varsigma)\phi_0'(\varsigma)$ at $1/\sqrt{-m}$ and $-1/\sqrt{-m}$; and

$$M_0 = \frac{(1-m^2)^2}{r[(1+m^2)(1+m^3)+2\xi(1-m^2)^2]}.$$

According to the Cauchy integral theorem, one may obtain

$$\frac{1}{2\pi i}\int_\gamma \frac{\phi_0(\eta)}{\eta-\varsigma}\,\mathrm{d}\eta = -\phi_0(\varsigma) \qquad |\varsigma| > 1, \qquad (23)$$

$$\frac{1}{2\pi i}\int_\gamma \frac{\overline{\phi_0(\eta)}}{\eta-\varsigma}\,\mathrm{d}\eta = 0 \qquad |\varsigma| > 1, \qquad (24)$$

$$\frac{1}{2\pi i}\int_\gamma \frac{\psi_0(\eta)}{\eta-\varsigma}\,\mathrm{d}\eta = -\psi_0(\varsigma) \qquad |\varsigma| > 1, \qquad (25)$$

$$\frac{1}{2\pi i}\int_\gamma \frac{\overline{\psi_0(\eta)}}{\eta-\varsigma}\,\mathrm{d}\eta = 0 \qquad |\varsigma| > 1. \qquad (26)$$

Substituting (23)–(26) into (9) and (10), one may derive $\phi_0(\zeta)$ and $\psi_0(\zeta)$ as

$$\phi_0(\varsigma) = -\frac{1}{2\pi i}\int_\gamma \frac{f_0\,\mathrm{d}\eta}{\eta-\varsigma} + \frac{1}{2\pi i}\int_\gamma \frac{\omega(\eta)}{\overline{\omega'(\eta)}}\overline{\phi_0'(\eta)}\frac{\mathrm{d}\eta}{\eta-\varsigma}, \qquad (27)$$

$$\psi_0(\varsigma) = -\frac{1}{2\pi i}\int_\gamma \frac{\overline{f_0}\,\mathrm{d}\eta}{\eta-\varsigma} + \frac{1}{2\pi i}\int_\gamma \frac{\overline{\omega(\eta)}}{\omega'(\eta)}\phi_0'(\eta)\frac{\mathrm{d}\eta}{\eta-\varsigma}. \tag{28}$$

According to the Cauchy theorem, we obtain that (for $|\zeta| > 1$)

$$\frac{1}{2\pi i}\int_\gamma \frac{\eta\,\mathrm{d}\eta}{\eta-\varsigma} = 0, \tag{29}$$

$$\frac{1}{2\pi i}\int_\gamma \frac{\mathrm{d}\eta}{\eta(\eta-\varsigma)} = -\frac{1}{\varsigma}, \tag{30}$$

$$\frac{1}{2\pi i}\int_\gamma \frac{\omega(\eta)}{\overline{\omega'(\eta)}}\frac{\mathrm{d}\eta}{\eta-\varsigma} = -\frac{m}{\varsigma} - M_0\frac{\varsigma}{\varsigma^2+m}, \tag{31}$$

$$\frac{1}{2\pi i}\int_\gamma \frac{\overline{\omega(\eta)}}{\omega'(\eta)}\frac{\mathrm{d}\eta}{\eta-\varsigma} = M_0\frac{\varsigma}{1+m\varsigma^2} - \frac{\overline{\omega}(1/\varsigma)}{\omega'(\varsigma)} + m\varsigma. \tag{32}$$

Substituting (21) and (29)–(31) into (27), we can show $\phi_0(\zeta)$ as

$$\begin{aligned}\phi_0(\varsigma) \;=\; & \left[\tfrac{1}{2}R(\sigma_1-\sigma_2)\,\mathrm{e}^{2i\alpha} - \tfrac{1}{4}R(\sigma_1+\sigma_2)\frac{rm}{r+2\xi}\right]\frac{1}{\varsigma} \\ & -M_0\tfrac{1}{4}R(\sigma_1-\sigma_2)\frac{\varsigma}{\varsigma^2+m} - \tfrac{1}{2}M_0\left[\frac{\overline{\phi_0'}\left(\frac{1}{\sqrt{-m}}\right)}{\varsigma-\sqrt{-m}} + \frac{\overline{\phi_0'}\left(\frac{-1}{\sqrt{-m}}\right)}{\varsigma+\sqrt{-m}}\right].\end{aligned} \tag{33}$$

It follows that

$$\begin{aligned}\phi_0'(\varsigma) \;=\; & -\left[\tfrac{1}{2}R(\sigma_1-\sigma_2)\,\mathrm{e}^{2i\alpha} - \tfrac{1}{4}R(\sigma_1+\sigma_2)\frac{rm}{r+2\xi}\right]\frac{1}{\varsigma^2} \\ & -M_0\tfrac{1}{4}R(\sigma_1+\sigma_2)\left[\frac{1}{\varsigma^2+m} - \frac{2\varsigma^2}{(\varsigma^2+m)^2}\right] \\ & +\frac{M_0}{2}\left[\frac{\overline{\phi_0'}\left(\frac{1}{\sqrt{-m}}\right)}{(\varsigma-\sqrt{-m})^2} + \frac{\overline{\phi_0'}\left(\frac{-1}{\sqrt{-m}}\right)}{(\varsigma+\sqrt{-m})^2}\right].\end{aligned} \tag{34}$$

Thus, we have

$$\begin{aligned}\phi_0'\left(\frac{1}{\sqrt{-m}}\right) \;=\; & \phi_0'\left(\frac{-1}{\sqrt{-m}}\right) \\ =\; & \frac{Rm(\sigma_1-\sigma_2)}{2}\left[\mathrm{e}^{2i\alpha} - \mathrm{e}^{-2i\alpha}M_0\frac{m(m^2+1)}{(m^2-1)^2}\right]\frac{1}{1-\left[M_0\frac{m(m^2+1)}{(m^2-1)^2}\right]^2} \\ & -\tfrac{1}{4}R(\sigma_1+\sigma_2)\left[\frac{rm^2}{r+2\xi} + M_0\frac{m(m^2+1)}{(m^2-1)^2}\right]\frac{1}{1+M_0\frac{m(m^2+1)}{(m^2-1)^2}}.\end{aligned} \tag{35}$$

Substituting (35) and (33) into (3), then using the boundary conditions given by (13)–(16), one derives

$$\phi(\varsigma) = \tfrac{1}{4}R(\sigma_1+\sigma_2)\varsigma + \left[\tfrac{1}{2}R(\sigma_1-\sigma_2)\,\mathrm{e}^{2i\alpha} - \tfrac{1}{4}R(\sigma_1+\sigma_2)\frac{rm}{r+2\xi}\right]\frac{1}{\varsigma} - M_0\frac{\varsigma}{\varsigma^2+m}\left[\tfrac{1}{4}R(\sigma_1+\sigma_2)+\rho\right], \tag{36}$$

where $\rho = \overline{\phi_0'}(1/\sqrt{-m}) = \overline{\phi_0'}(-1/\sqrt{-m})$.

Similarly, the substitution of (22), (29), (30), (32) and (35) into (28) may give the expression for $\psi_0(\varsigma)$, then using the boundary conditions of equations (13)–(16), one derives from (4) that

$$\psi(\varsigma) = -\tfrac{1}{2}R(\sigma_1-\sigma_2)\,\mathrm{e}^{-2i\alpha}\varsigma + \tfrac{1}{4}R(\sigma_1+\sigma_2)\left[m\varsigma - \frac{1}{\varsigma} - \frac{\overline{\omega}(1/\varsigma)}{\omega'(\varsigma)} + \frac{M_0\varsigma}{1+m\varsigma^2}\right] - \frac{\overline{\omega}(1/\varsigma)}{\omega'(\varsigma)}\phi_0'(\varsigma) + \frac{M_0\varsigma}{1+m\varsigma^2}\overline{\rho}. \tag{37}$$

Equations (36) and (37) are the complex stress functions for the problem of an infinite plate containing a central leaf-shaped notch.

The stress field can be obtained from the complex stress functions with

$$\sigma_x + \sigma_y = 4\mathrm{Re}[\Phi(\varsigma)], \tag{38}$$

$$\sigma_x - \sigma_y + 2i\tau_{xy} = \frac{2}{\omega'(\varsigma)}[\Phi'(\varsigma)\overline{\omega(\varsigma)} + \Psi(\varsigma)\omega'(\varsigma)], \tag{39}$$

where $\Phi(\varsigma) = \phi'(\varsigma)/\omega'(\varsigma)$, and $\Psi(\varsigma) = \psi'(\varsigma)/\omega'(\varsigma)$. The solutions to (38) and (39) will give the stress distribution with respect to ζ, which may especially show the stress field in the vicinity of the notch root for a leaf-shaped notch. Note that the conformal mapping formulas of (1) and (2) provide the unique transformation between the z-plane and the ζ-plane, i.e. there is a unique correlation between a point on the ζ-plane and a relevant point on the z-plane. The most important points are $\zeta = \pm 1$, which correspond to $z = \pm a$ by (1), or $z = \pm a(1+\xi)$ by (2). Let ξ be 0, then a leaf-shaped profile becomes a lip-shaped crack with sharp tips. Consequently, the stress field at the tip of a lip-shaped crack can be derived. Figures 4(a)–(d) show the distribution of σ_θ for different values of ξ, indicating that the distribution of σ_θ has strong singularity characteristics as the value of ξ tends to zero.

It is known that, if the crack width is zero, the singularity order of the stress field at the crack tip is $-\frac{1}{2}$. However, if the crack width is not zero ($b > 0$) but with sharp tips, the singularity order of the stress field can be analyzed by means of the above complex stress functions by reducing the value of ξ to zero.

Referring to (38) and (39), σ_y is the sum of the following three terms: $2\mathrm{Re}[\Phi(\varsigma)]$, $\mathrm{Re}[\Psi(\varsigma)]$ and $\mathrm{Re}[\Phi'(\varsigma)(\overline{\omega(\varsigma)}/\omega'(\varsigma))]$. Based on the theoretical analysis and the numerical calculations it is evident that all of the three terms become infinite at the tips of a lip-shaped crack. The singularity intensity of the third term is the most predominant, and that of the other two terms have a comparatively small effect. Figure 5 shows this tendency in terms of σ_θ versus ζ_1, with $\alpha = 0$. It is obvious that the singularity order of σ_y is dominated by the term of $\mathrm{Re}[\Phi'(\varsigma)(\overline{\omega(\varsigma)}/\omega'(\varsigma))]$, i.e. the third term.

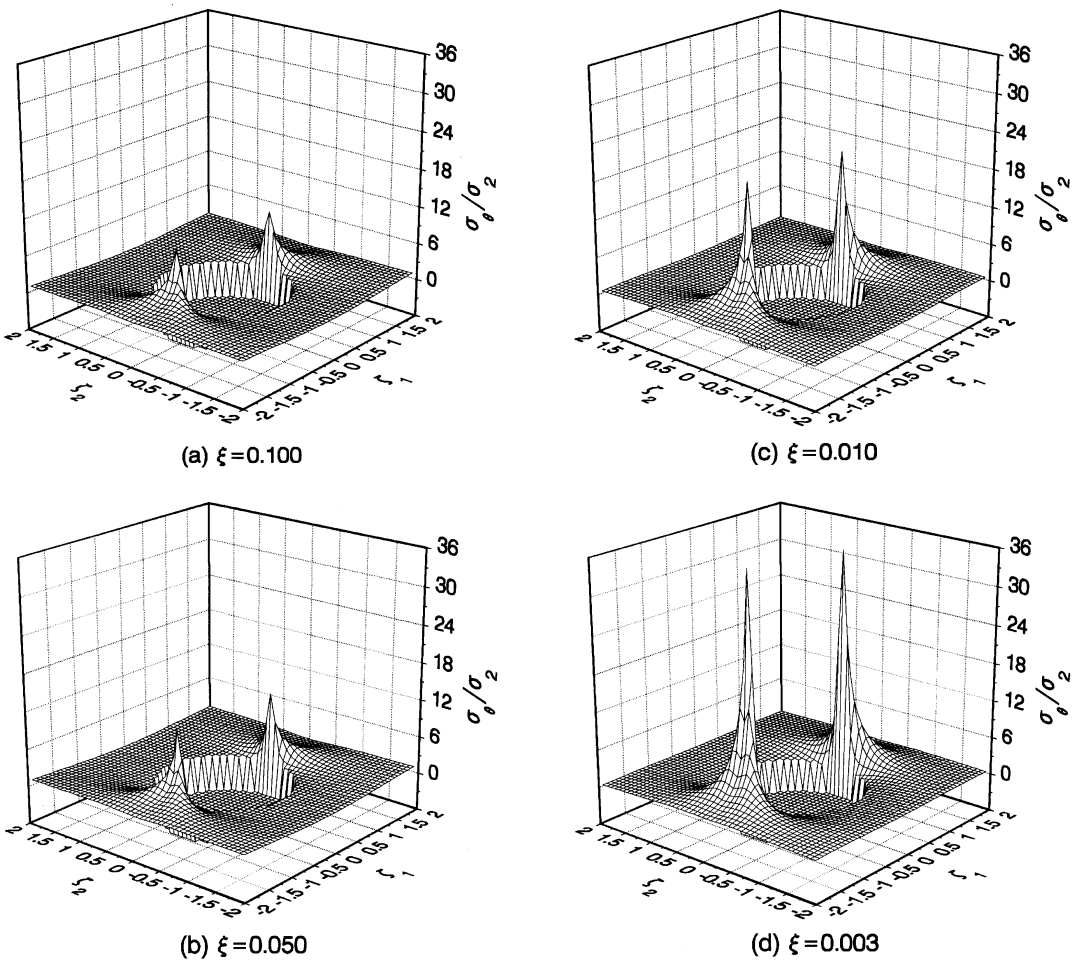

Figure 4. Stress field for leaf-shaped notch in ζ-plane at different values of ξ, with $\alpha = 0$, $\sigma_1 = 0$, $\sigma_2 = 1$, $a = 1$, and $b = 0.1$.

Consider the singularity order of $\Phi'(\zeta)$ and $\overline{\omega(\varsigma)}/\omega'(\varsigma)$ along the real axis at $\zeta = \pm 1$, respectively. For convenience in the following discussion, we let

$$\varsigma = \frac{1}{\lambda} + 1. \tag{40}$$

Thus $\Phi'(\varsigma)$ and $\overline{\omega(\varsigma)}/\omega'(\varsigma)$ can be rewritten as a function of λ

$$\frac{\overline{\omega[\varsigma(\lambda)]}}{\omega'[\varsigma(\lambda)]} = F(\lambda), \tag{41}$$

$$\Phi'[\varsigma(\lambda)] = G(\lambda). \tag{42}$$

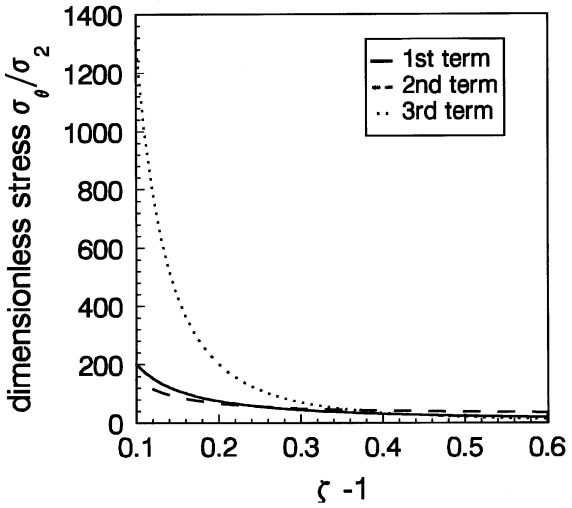

Figure 5. Stress singularity tendency of the three terms of σ_θ.

It is clear that $F(\lambda)$ and $G(\lambda)$ have the same singularity order as $\Phi'(\varsigma)$ and $\overline{\omega(\varsigma)}/\omega'(\varsigma)$ respectively, while the singularity points shift to $\pm\infty$. If ξ is zero, $F(\lambda)$ has the form

$$F(\lambda) = \frac{2(m+1)^2\lambda^9 + 4(2m+3)(m+1)\lambda^8 + O(\lambda^7)}{2(m-1)^2\lambda^8 + O(\lambda^7)}, \tag{43}$$

where $O(\lambda^i)$ represents the polynome with the order of λ^i. It is seen that when λ tends to infinity the singularity order of $F(\lambda)$ can be derived as

$$\begin{cases} F(\lambda) \sim O(\lambda) & \text{for } m \neq -1 \\ F(\lambda) \to 0 & \text{for } m = -1. \end{cases} \tag{44}$$

Note that $m = -1$ corresponds to $a/b \to 0$. When ξ is zero, the shape of the notch is sharp and the stress singularity inevitably exists. For simplicity in the discussion of stress singularity at the sharp notch tip, we set $\alpha = 0$ and consider two cases: (a) $\sigma_1 = 0$, $\sigma_2 = \sigma$, and (b) $\sigma_1 = \sigma$, $\sigma_2 = 0$.

For case (a), substitution of $r = 1/(1+m)$ and (40) into (42) gives

$$\begin{aligned} \Phi'[\varsigma(\lambda)] &= G(\lambda) \\ &= \tfrac{1}{4}\sigma[(m^7 + 3m^6 + 2m^5 + 6m^4 + 11m^3 + 5m^2 + 2m + 2)\lambda^6 \\ &\quad +(m^7 + 3m^6 + 3m^5 + 15m^4 + 31m^3 + 13m^2 + 5m + 9)\lambda^5 \\ &\quad +O(\lambda^4)]\left[\frac{(m-1)^2}{1+m}\lambda^5 + O(\lambda^4)\right]^{-1}. \end{aligned} \tag{45}$$

From the above equation, it is seen that when λ tends to infinity and $m \neq -1$, the singularity order of $\Phi'[\varsigma(\lambda)]$ is 1. For the extreme situation that $m = -1$, there exists

$$\Phi'[\varsigma(\lambda)]|_{\lambda\to\infty} \to 0, \tag{46}$$

which implies that the stress is zero at the notch tip and that the stress singularity is not relevant.

For case (b), substitution of $r = 1/(1+m)$ and (40) into (42) gives

$$\begin{aligned}\Phi'[\varsigma(\lambda)] &= G(\lambda) \\ &= \tfrac{1}{2}\sigma[(m^7 - m^6 + 4m^4 - m^3 - 3m^2)\lambda^6 \\ &\quad +(m^7 - m^6 + 3m^5 + 15m^4 - m^3 - 7m^2 + 5m + 1)\lambda^5 + O(\lambda^4)] \\ &\quad \times[(2m^3 - 2m^2 - 2m + 2)\lambda^5 + (m^3 - 5m^2 - 5m + 9)\lambda^4 + O(\lambda^3)]^{-1}. \qquad (47)\end{aligned}$$

It is seen that when λ tends to infinity for $m \neq -1$ and $m \neq 0$, the singularity order of $\Phi'[\varsigma(\lambda)]$ is 1. For the extreme situation that $m = -1$ and $m \neq 0$, one may show

$$\Phi'[\varsigma(\lambda)]|_{\lambda\to\infty} \to O(\lambda^0). \qquad (48)$$

Based on the above analyses, we may deduce the singularity order of σ_y on the ζ-plane, which is caused by the joint effect of $\Phi'(\zeta)$ and $\overline{\omega(\varsigma)}/\omega'(\varsigma)$. It is noticed that the singularity order of $\Phi'(\zeta)$ and $\overline{\omega(\varsigma)}/\omega'(\varsigma)$ at $\zeta \to 1$ corresponds to the singularity order of $\Phi'(\lambda)$ and $\overline{\omega(\lambda)}/\omega'(\lambda)$ at $\lambda \to \infty$. From (43)–(48), we obtain that the singularity order of σ_y on the ζ-plane is $|2|$ for $m \neq -1$ and is 0 for $m = -1$.

The next step is to derive the singularity order on the z-plane. For this purpose, we may use the relation of $r = 1/(1+m)$ and rewrite (2) as

$$a\varsigma^4 - 2\omega(1+m)\varsigma^3 + a(m^2 + 4m + 1)\varsigma^2 - 2\omega m(1+m)\varsigma + am^2 = 0. \qquad (49)$$

We can see that the power order of ζ is 4 and that of ω is 1, i.e. the power order of ω is one fourth of that of ζ. Therefore, we may state that the singularity order of σ_y on the z-plane is $|\frac{1}{2}|$ for $m \neq -1$ and is 0 for $m = -1$. Again note that when $m = -1$, i.e. $a = 0$, the notch crack does not exist. Otherwise when $m \neq -1$, i.e. a sharp notch crack with different sizes in width, the singularity order of the stress field always remains $-\frac{1}{2}$. This result confirms that the singularity order of a notch crack is the same as that of an ordinary crack and that the K-theory in terms of stress singularity characteristics is physically valid.

4. Conclusions

By using the conformal mapping method, the distribution and the singularity characteristics of an infinite thin plate with a central lip-shaped crack subjected to remote boundary biaxial loading was studied. The deviation was performed by taking advantage of a leaf-shaped configuration. The singularity order of the crack-tip stress field remains $-\frac{1}{2}$, which is not affected by the change of notch-crack width. Thus, the validity of the Williams stress field is confirmed and the K-method can be reasonably applied for the real crack with a certain amount in crack width other than the ideal geometric one.

Acknowledgments

This paper was supported by the National Outstanding Youth Scientific Award of China, the National Natural Science Foundation of China and the Chinese Academy of Sciences.

References

Baskes, M.I. (1975). A simplified prediction of K_{IC} from tensile data. *Engineering Fracture Mechanics* **7**, 249–251.

Bowie, O.L. (1956). Analysis of an infinite plate containing radial cracks originating from the boundary of an internal circular hole. *Journal of Mathematical Physics* **35**, 60–71.

Hong, Y.S., Miller, K.J. and Brown, M.W. (1991). Complex stress functions and plastic zone sizes for notch cracks subjected to various loading conditions. *Fatigue & Fracture of Engineering Materials & Structures* **14**, 237–258.

Hui, Y. and Ruida, A. (1995). Why K? Higher-order singularities and small-scale yielding. *International Journal of Fracture* **72**, 97–120.

Irwin, G.R. (1957). Analysis of stresses and strains near the end of a crack traversing a plate. *Journal of Applied Mechanics* **24**, 361–364.

Muskhelishvili, N.I. (1954). *Some Basic Problems of the Mathematical Theory of Elasticity*, 4th edn. Noordhoff, Groningen.

Prakash, V., Freund, L.B. and Clifton, R.L. (1992). Stress wave radiation from a crack tip during dynamic initiation. *Journal of Applied Mechanics* **59**, 356–365.

Schijve, J. (1982). The stress intensity factor of small cracks at notches. *Fatigue & Fracture of Engineering Materials & Structures* **5**, 77–90.

Wang, Y.S. and Wang, D. (1992). Moving dislocation model of propagating self-similar interface crack. *International Journal of Fracture* **54**, 9–14.

Williams, M.L. (1952). Stress singularities resulting from various boundary conditions in angular corners of plates in extension. *Journal of Applied Mechanics* **19**, 526–528.

Williams, M.L. (1957). On the stress distribution at the base of a stationary crack. *Journal of Applied Mechanics* **24**, 109–114.

Xiao, S.T., Brown, M.W. and Miller, K.J. (1985). Stress intensity factor for cracks in notched finite plates subjected to biaxial loading. *Fatigue & Fracture of Engineering Materials & Structures* **8**, 349–372.

Zhao, Y.P. (1996). The advances of studies on the dynamic initiation of cracks. *Advances in Mechanics* **26**, 362–378. (In Chinese).